Molecular Pharmacology Fast Forward. Published on September 27, 2022 as DOI: 10.1124/molpharm.122.000539
This article has not been copyedited and formatted. The final version may differ from this version.

Cancer-type organic anion transporting polypeptide 1B3 (Ct-OATP1B3) is localized in lysosomes and mediates resistance against kinase inhibitors

Bastian Haberkorn[1], Stefan Oswald[2], Niklas Kehl[1], Arne Gessner[1], R. Verena Taudte[1], Jan Philipp Dobert[3], Friederike Zunke[3], Martin F. Fromm[1] and Jörg König[1#]

Institute of Experimental and Clinical Pharmacology and Toxicology, Friedrich-Alexander-Universität Erlangen-Nürnberg, Erlangen, Germany

Molecular Pharmacology Fast Forward. Published on September 27, 2022 as DOI: 10.1124/molpharm.122.000539
This article has not been copyedited and formatted. The final version may differ from this version.

Running Title: Cancer-type OATP1B3 and kinase inhibitor resistance

[#]**Correspondence:** Prof. Dr. Jörg König
Institute of Experimental and Clinical Pharmacology and Toxicology
Clinical Pharmacology and Clinical Toxicology
Friedrich-Alexander-Universität Erlangen-Nürnberg
Fahrstrasse 17
91054 Erlangen
Germany
Joerg.koenig@fau.de
Tel: ++49-9131-8522077
Fax: ++49-9131-8522773

Number of text pages: **38**

Number of tables: **0**

Number of figures: **7**

Number of references: **59**

Number of words:

Abstract: **236**

Introduction: **733 (with references)**

Discussion: **1164 (with references)**

Abbreviations: ABC, ATP-binding cassette; AF568, Alexa Fluor™ 568 antibody; AF647, Alexa Fluor™ 647 antibody; BSP, bromosulfophthalein; CCK-8, Cell Counting Kit-8; CRC, colorectal carcinoma; Ct-OATP1B3, cancer-type organic anion transporting polypeptide 1B3; $E_2$17βG, estradiol-17β-glucuronide;FDA, Food and Drug Administration; HEK293, human embryonic kidney 293; HMG-CoA, 3-hydroxy-3-methylglutaryl-coenzyme A; LAMP1, lysosomal associated membrane protein 1; Lt-OATP1B3, liver-type organic anion transporting polypeptide 1B3; OG, Oregon Green™ 488 carboxylic acid succinimidyl ester; OICE, Optical Imaging Center Erlangen; SLC, solute carrier

Molecular Pharmacology Fast Forward. Published on September 27, 2022 as DOI: 10.1124/molpharm.122.000539
This article has not been copyedited and formatted. The final version may differ from this version.

Abstract

Cancer-type organic anion transporting polypeptide 1B3 (Ct-OATP1B3), a splice variant of the hepatic uptake transporter OATP1B3 (liver-type; Lt-OATP1B3), is expressed in several tumor entities including colorectal carcinoma (CRC) and breast cancer. In CRC, high OATP1B3 expression has been associated with reduced progression-free and overall survival. Several kinase inhibitors used for antitumor treatment are substrates and/or inhibitors of OATP1B3 (e.g. encorafenib, vemurafenib). The functional importance of Ct-OATP1B3 has not been elucidated so far. HEK293 cells stably overexpressing Ct-OATP1B3 protein were established and compared with control cells. Confocal laser scanning microscopy, immunoblot, and proteomics-based expression analysis demonstrated that Ct-OATP1B3 protein is intracellularly localized in lysosomes of stably-transfetced cells. Cytotoxicity experiments showed that cells recombinantly expressing the Ct-OATP1B3 protein were more resistant against the kinase inhibitor encorafenib compared to control cells [e.g. encorafenib (100 µM) survival rates: 89.5% vs. 52.8%]. In line with these findings, colorectal cancer DLD1 cells endogenously expressing Ct-OATP1B3 protein had poorer survival rates when the OATP1B3 substrate bromosulfophthalein (BSP) was coincubated with encorafenib or vemurafenib compared to the incubation with the kinase inhibitor alone. This indicates a competitive inhibition of Ct-OATP1B3-mediated uptake into lysosomes by BSP. Accordingly, mass spectrometry-based drug analysis of lysosomes showed a reduced lysosomal accumulation of encorafenib in DLD1 cells additionally exposed to BSP. These results demonstrate that Ct-OATP1B3 protein is localized in the lysosomal membrane and can mediate transport of certain kinase inhibitors into lysosomes revealing a new mechanism of resistance.

Molecular Pharmacology Fast Forward. Published on September 27, 2022 as DOI: 10.1124/molpharm.122.000539
This article has not been copyedited and formatted. The final version may differ from this version.

Significance Statement

We describe the characterization of a splice variant of the liver-type uptake transporter OATP1B3 expressed in several tumor entities. This variant is localized in lysosomes mediating resistance against kinase inhibitors which are substrates of this transport protein by transporting them into lysosomes and thereby reducing the cytoplasmic concentration of these antitumor agents. Therefore, the expression of the Ct-OATP1B3 protein is associated with a better survival of cells revealing a new mechanism of drug resistance.

1. Introduction

Transport proteins are important for the uptake, distribution, and excretion of xenobiotics, drugs, and endogenous substances in normal and cancerous tissues (Pizzagalli et al., 2021; Robey et al., 2018). Export proteins usually belong to the superfamily of ABC (ATP-binding cassette) transporters (Locher, 2016; Moitra and Dean, 2011), whereas uptake transporters are members of the SLC (solute carrier) transporter superfamily (Pizzagalli et al., 2021). Additionally to their expression in all healthy tissues including intestine, kidney, and liver, ABC and SLC transporters are also expressed in several cancerous tissues mediating the uptake or export of drugs or endogenous substrates into or out of cancer cells (Al-Abdulla et al., 2019; Robey et al., 2018; Zhang and Wang, 2020). Remarkably, during antitumor therapy ABC transporters in particular have been characterized as important mediators of drug resistance when they are overexpressed in cancerous tissues (Robey et al., 2018), whereas in this context, the role of SLC transporters is currently under intensive investigation (Huang et al., 2020; Krchniakova et al., 2020; Neul et al., 2016; Sun et al., 2020).

Molecular Pharmacology Fast Forward. Published on September 27, 2022 as DOI: 10.1124/molpharm.122.000539
This article has not been copyedited and formatted. The final version may differ from this version.

The focus of this study is on a variant of the SLCO/SLC21 family member organic anion transporting polypeptide 1B3 (OATP1B3, gene symbol *SLCO1B3*). OATP1B3 has been characterized as an uptake transporter predominantly localized in the basolateral membrane of human hepatocytes (König et al., 2000). Several endogenous substances as well as widely prescribed drugs have been identified as substrates of this transporter (Fahrmayr et al., 2010; Roth et al., 2012; Seithel et al., 2008). Transported drugs include HMG-CoA reductase inhibitors (statins), antibiotics and several antitumor therapeutic agents such as methotrexate, paclitaxel, and kinase inhibitors (e.g. vemurafenib) (Kayesh et al., 2021; Zimmerman et al., 2013).

In 2001, Abe and coworkers reported that OATP1B3 is also expressed in several cancerous tissues and cancer-derived cells (Abe et al., 2001). Nagai and colleagues finally demonstrated that not the liver-type OATP1B3 protein (Lt-OATP1B3), but an isoform of Lt-OATP1B3 protein, termed Ct-OATP1B3 protein (cancer-type OATP1B3) is expressed in human cancerous tissues (Nagai et al., 2012). This isoform results from alternative splicing of the *SLCO1B3* gene with the *Ct-SLCO1B3* mRNA possessing a unique first exon (called exon 1*), which originates from an alternative transcriptional start site located in intron 3 (Figure 1) of the *SLCO1B3* gene (Nagai et al., 2012). Ct-OATP1B3 protein encoded by the alternatively spliced *Ct-SLCO1B3* mRNA lacks the first 28 amino acids of Lt-OATP1B3 [Figure 1 (Sun et al., 2014)]. Sun and coworkers could discriminate between *Lt-* and *Ct-SLCO1B3* mRNA and demonstrated that *Ct-SLCO1B3* mRNA is expressed in 87.2% of investigated colorectal cancer tissues, but only in 2.6% of the adjacent healthy tissues. So far, in vitro data regarding Ct-OATP1B3 protein transport function and subcellular localization are controversial (Imai et al., 2013; Sun et al., 2014; Thakkar et al., 2013). Interestingly, it has been demonstrated that the aminoterminal region of the

Molecular Pharmacology Fast Forward. Published on September 27, 2022 as DOI: 10.1124/molpharm.122.000539
This article has not been copyedited and formatted. The final version may differ from this version.

OATP1B3 protein, which is present in Lt-OATP1B3, but absent in Ct-OATP1B3 (Figure 1C) seems to be important for the correct insertion of Lt-OATP1B3 in the plasma membrane (Chun et al., 2017).

Expression of *Ct-SLCO1B3* mRNA or Ct-OATP1B3 protein has been confirmed in different cancerous tissues including colorectal (Abe et al., 2001; Lee et al., 2008), gastric (Abe et al., 2001), breast (Muto et al., 2007), prostate (Hamada et al., 2008; Pressler et al., 2011), and pancreatic cancer (Hays et al., 2013; Kounnis et al., 2011). Interestingly, a study with 278 colorectal tumor samples demonstrated a higher *Ct-SLCO1B3* mRNA expression in lower stage tumors (Lockhart et al., 2008), whereas Lee et al. found no correlation between tumor stage and *Ct-SLCO1B3* mRNA expression (Lee et al., 2008). Furthermore, some studies found that a high expression of Ct-OATP1B3 protein is associated with a better overall survival of colorectal cancer or endometrial cancer patients (Lockhart et al., 2008; Ogane et al., 2013; Tang et al., 2021), whereas other studies found that a high expression of *Ct-SLCO1B3* mRNA is associated with a reduced progression-free survival in patients with advanced and metastatic colorectal cancer (Teft et al., 2015). Recently a high *SLCO1B3* gene expression was associated with lower overall survival in patients with colorectal cancer (Zhi et al., 2021). Taken together, the cancer-type variant of OATP1B3 protein is expressed in several cancerous tissues, but the localization, transport function, and possible role of expression needs to be elucidated. Therefore, the aim of this exploratory study is to gain insights into the subcellular localization, transport function, and possible functional role of Ct-OATP1B3.

2. Materials and Methods

2.1. Materials

Molecular Pharmacology Fast Forward. Published on September 27, 2022 as DOI: 10.1124/molpharm.122.000539
This article has not been copyedited and formatted. The final version may differ from this version.

[^{3}H]-bromosulfophthalein (BSP, 14 Ci/mmol) was obtained from HARTMANN ANALYTIK GmbH (Braunschweig, Germany). [^{3}H]-estradiol-17β-glucuronide ($E_2$17βG, 50 Ci/mmol) was purchased from American Radiolabeled Chemicals, Inc. (St. Louis, USA). Stably-labelled [$^2H_3$]-clopidogrel was purchased from @rt molecule (Poitiers, France). Unlabeled BSP was from AppliChem GmbH (Darmstadt, Germany), unlabeled $E_2$17βG and the ProteoExtract® Native Membrane Protein Extraction Kit were from Sigma Aldrich (St. Louis, USA). Regorafenib was purchased from LC Laboratories (Woburn, USA). Encorafenib and vemurafenib were from MedChemtronica AB (Sollentuna, Sweden). Minimum essential medium, DMEM/F12 (1:1), RPMI Medium 1640, Dulbecco's phosphate buffered saline, fetal bovine serum, hygromycin B (50 mg/mL), Penicillin streptomycin solution, 0.05%-trypsin-EDTA solution, Pierce™ BCA Protein Assay Kit, CellLight® Lysosomes-RFP, BacMam 2.0 and the SYTOX® Green nucleic acid stain were obtained from Thermo Fisher Scientific (Dreieich, Germany). The NucleoSpin® RNA Plus Kit was obtained from MACHEREY-NAGEL GmbH & Co. KG (Düren, Germany). The iScript™ cDNA Synthesis Kit was from Bio-Rad Laboratories GmbH (München, Germany). The Minute™ Plasma Membrane Protein Isolation and Cell Fractionation Kit was purchased from Invent Biotechnologies, Inc. (Plymouth, USA). 6-well, 12-well and 96-well cell culture plates were from Greiner Bio-One (Frickenhausen, Germany). Oregon Green™ 488 carboxylic acid, succinimidyl ester (OG) was obtained from Invitrogen (Rockford, USA). The LightCycler® FastStart DNA Master^{PLUS} SYBR® Green I Kit was obtained from Roche Diagnostics GmbH (Mannheim, Germany). SPY555-DNA (SPY™ dyes series) was from Spirochrome AG (Stein am Rhein, Switzerland) and the pmScarlet-1_peroxisome_C1 plasmid (RRID:Addgene_85065; Addgene, Waterhouse, USA) was kindly provided by the Optical Imaging Center Erlangen (OICE). The μ-Slide 8-well glass bottom arrays were obtained by ibidi

Molecular Pharmacology Fast Forward. Published on September 27, 2022 as DOI: 10.1124/molpharm.122.000539
This article has not been copyedited and formatted. The final version may differ from this version.

GmbH (Gräfeling, Germany). The CCK-8 Assay was purchased from GERBU Biotechnik GmbH (Heidelberg, Germany).

2.2. Antibodies

Polyclonal rabbit anti-human OATP1B3 antiserum (SKT) directed against the carboxyterminal end of the human OATP1B3 protein (König et al., 2000) was obtained from the Division of Tumor Biochemistry of the German Cancer Research Center (Heidelberg, Germany). The goat anti-rabbit IgG-horseradish peroxidase-labeled antibody (RRID:AB_2650489) was purchased from GE Healthcare Life Sciences (Buckinghamshire, UK). The goat anti-mouse IgG Alexa Fluor™ Plus 647 antibody (AF647; RRID:AB_2633277), the Alexa Fluor™ 568 goat anti-rabbit IgG antibody (AF568; RRID:AB_143157) and the the goat anti-mouse IgG (H+L) secondary antibody, HRP antibody (RRID:AB_2533947) were from Thermo Fisher Scientific (Dreieich, Germany). The Anti-alpha 1 Sodium Potassium ATPase antibody (RRID:AB_306023) was from Abcam plc. (Cambridge, UK). The monoclonal mouse anti-pan cadherin antibody (RRID:AB_476826), the mouse anti-β-actin monoclonal antibody (RRID:AB_476743) and the anti-LAMP1 antibody produced in rabbit (RRID:AB_477157) were purchased from Sigma-Aldrich (St. Louis, USA).

2.3. Cell culture

Human embryonic kidney 293 (HEK293; RRID:CVCL_0045) cells were obtained from ATCC and incubated at 37°C and 5% CO_2. The cell culture medium was minimum essential medium, supplemented with 10% heat-inactivated fetal bovine serum, 100 U/mL penicillin and 100 µg/mL streptomycin. For antibiotic selection, hygromycin B (250 µg/mL) was added. The stable-transfected cell lines were routinely checked for expression of the respective transport protein. DLD1 (RRID:CVCL_0248) and T84 cells (RRID:CVCL_0555) were kindly provided by PD

Molecular Pharmacology Fast Forward. Published on September 27, 2022 as DOI: 10.1124/molpharm.122.000539
This article has not been copyedited and formatted. The final version may differ from this version.

Dr. Britzen-Laurent and Prof. Dr. Naschberger (Department of Surgery, Erlangen, Germany). All human cell lines have been authenticated using STR (or SNP) profiling within the last three years and the experiments were performed with mycoplasma-free cells. For DLD1 cells RPMI 1640 medium and for T84 cells DMEM/F12 (1:1) medium was used, both supplemented with 10% heat-inactivated fetal bovine serum, 100 U/mL penicillin and 100 µg/mL streptomycin. Subcultivation was done twice a week using trypsin 0.05%-EDTA 0.02% solution.

2.4. Generation of stably-transfected HEK-Ct-OATP1B3 and HEK-Kz-Ct-OATP1B3 cells

For the amplification of the *Ct-SLCO1B3* cDNA, synthesized sscDNA of human colon tumor total RNA served as template, using oCt-OATP1B3-5'-For (5'-aactagcagatgttcttggcag-3') and oOATP1B3-RT-Rev2 (5'-gcatagacttatccattggtcc-3') as primers. Subsequent to TOPO-TA cloning, the *Ct-SLCO1B3* cDNA was cloned into the expression vector pcDNA3.1 Hygro(-) resulting in the plasmid pCt-SLCO1B3.31_Hygro. To introduce the Kozak sequence around the start ATG, the pCt-SLCO1B3.31_Hygro plasmid and the primer pair oCt-OATP1B3.Kozak.For (5'-gccgccaccatgttcttggcagc-3') and oOATP1B3-RT-Rev2 were used to amplify a modified cDNA. This cDNA was cloned into the vector pcR2.1.Topo and subcloned into the expression vector pcDNA3.1 Hygro(-) resulting in the plasmid pKozak-Ct-SLCO1B3.31_Hygro. Before transfection, all cDNAs were sequenced and both plasmids contain a cDNA encoding the same Ct-OATP1B3 protein. Stable transfectants expressing the Ct-OATP1B3 protein were established in the same way as described before by Taghikhani et al. (Taghikhani et al., 2019), resulting in the HEK293 cell lines HEK-Ct-OATP1B3 and HEK-Kz-Ct-OATP1B3.

2.5. Quantitative polymerase chain reaction

Molecular Pharmacology Fast Forward. Published on September 27, 2022 as DOI: 10.1124/molpharm.122.000539
This article has not been copyedited and formatted. The final version may differ from this version.

Total RNA was isolated using the NucleoSpin® RNA Plus Kit according to the manufacturers protocol. The concentration of the isolated RNA was photometricly measured. The iScript™ cDNA Synthesis Kit was used according to the manufacturers protocol to generate the first-strand cDNA using 1 µg total RNA per sample. For the qRT-PCR reaction the LightCycler® FastStart DNA Master^{PLUS} SYBR® Green I Kit was used. Each sample consisted of 5 µL purified water, 2 µL solution I (Kit included), 1 µL forward- and reverse-primer, respectively and 1 µL template sscDNA. Subsequently to the initial 10 min denaturation step at 95°C the DNA was amplified during 45 cycles of 10 s denaturation at 95°C, 10 s annealing at 64°C and 30 s elongation at 72°C. The expression of each sample was calculated via linear regression and normalised to the respective expression of the housekeeping gene *β-actin*.

2.6. Immunoblot analysis

The immunoblot analysis was performed as described earlier.(Taghikhani et al., 2020) A protein amount of 30 µg was used for the whole cell homogenate. The plasma membrane fractions and cytosolic fractions were adjusted to an amount of 10 µg protein. For the detection of the OATP1B3 protein, the membrane was incubated with the polyclonal antiserum SKT (1:500) at 4°C overnight. To detect the binding of the primary antibody, the goat anti-rabbit IgG-horseradish peroxidase-labeled antibody (1:10 000) served as secondary antibody. To control sample loading either the monoclonal mouse anti-human β-actin primary antibody (1:10 000) or the monoclonal mouse anti-pan cadherin antibody (1:2000) was used. The goat anti-mouse IgG-horseradish peroxidase-labeled antibody (1:2000) was used as secondary antibody. For the analysis of the enriched lysosomal fraction, 10 µg

Molecular Pharmacology Fast Forward. Published on September 27, 2022 as DOI: 10.1124/molpharm.122.000539
This article has not been copyedited and formatted. The final version may differ from this version.

protein was used and staining with the rabbit anti-LAMP1 antibody (1:1000) served as loading control.

2.7. Immunofluorescence microscopy

Cells were seeded at an initial cell number of 3 x 10^5 cells per well on poly-D-lysine coated object slides. After 24 h, cells were fixed using 70% ice-cold methanol solution and permeabilized with 0.4% Triton 100-PBS solution. To block the fixed cells, 2% BSA-water solution was added and the cells were incubated with the polyclonal antiserum SKT (1:500) and the anti-alpha 1 sodium potassium ATPase antibody (1:500) overnight at 4°C. AF568 and AF647 were used as secondary antibodies (1:2000). The nuclei were counterstained with SYTOX® Green nucleic acid stain. Microscopy was performed on the Zeiss Spinning Disc Axio Observer Z1 at the OICE (Erlangen, Germany).

2.8. Subcellular fractionation

To separate the plasma membrane fraction from the cytosolic fraction of the stable transfectants, 1 x 10^7 cells were seeded on 10 cm plates. Twenty-four hours later, protein expression was induced with the addition of sodium butyrate (final concentration 10 mM). 48 h after seeding, cells were washed with 2 mL PBS and after the addition of 1.5 mL PBS, cells were transferred into a 2 mL microcentrifuge tube and centrifuged for 5 min at 600 x g at 4°C. For isolation, the Minute™ Plasma Membrane Protein Isolation and Cell Fractionation kit was used. The plasma membrane fraction was finally dissolved in 50 µL of the extraction buffer II of the ProteoExtract® Native Membrane Protein Extraction kit. For immunoblot analysis, the plasma membrane fraction was lysed in 0.2% SDS solution containing the cOmplete™ Tablets (Roche Diagnostics GmbH, Mannheim, Germany) as proteinase inhibitor cocktail.

Molecular Pharmacology Fast Forward. Published on September 27, 2022 as DOI: 10.1124/molpharm.122.000539
This article has not been copyedited and formatted. The final version may differ from this version.

2.9. Lysosome enrichment

The lysosome fraction was isolated according to Mazzulli et al. (Mazzulli et al., 2011). For each sample, cells from three 10 cm plates (1 x 10^7 cells/plate) were pooled and resuspended in 600 µL sucrose-HEPES buffer (0.25 M sucrose, 10 mM HEPES pH 7.4, 0.1 M EDTA). The cell suspension was homogenized using the B.Braun Potter S homogenizer and subsequently centrifuged for 5 min at 6800 x g and 4°C. The supernatant was saved and the pellet was again resuspended in 600 µL sucrose-HEPES buffer and homogenization and centrifugation was repeated. Both supernatants were combined and centrifuged for 10 min at 17 000 x g and 4°C. The supernatant was removed and the pellet, containing the enriched lysosomal fraction was saved until further use. For immunoblot analysis, the final pellet was lysed in 0.2% SDS solution containing proteinase inhibitor cocktail.

2.10. Protein quantification by LC-MS/MS

Protein abundance of OATP1B3 and Na/K-ATPase as reference protein was determined using a validated LC-MS/MS-based targeted proteomics assay as described elsewhere (Drozdzik et al., 2019). To isolate the crude membrane protein fraction, the cell pellets from five 75 cm² cell culture flasks per sample were pooled and isolated with the ProteoExtract® Native Membrane Protein Extraction kit (Merck KGaA, Darmstadt, Germany) according to the manufacturer's protocol. The protein concentration of the obtained crude membrane fractions was determined with the BCA assay. To analyze the amount of OATP1B3 protein in the plasma membrane fraction the Minute™ Plasma Membrane Protein Isolation and Cell Fractionation kit was used as mentioned above. If necessary, membrane fractions were adjusted to a maximum protein amount of 2 mg/mL.

Molecular Pharmacology Fast Forward. Published on September 27, 2022 as DOI: 10.1124/molpharm.122.000539
This article has not been copyedited and formatted. The final version may differ from this version.

Subsequently, 100 µL of each membrane fraction was mixed with 10 µL dithiothreitol (200 mM; Sigma-Aldrich, Taufkirchen, Germany), 40 µL ammonium bicarbonate buffer (50 mM, pH 7.8; Sigma-Aldrich, Taufkirchen, Germany), and 10 µL ProteaseMAX™ (1% m/v; Promega, Mannheim, Germany) and incubated for 20 min at 60°C (denaturation). After cooling down, 10 µL iodoacetamide (400 mM; Sigma-Aldrich, Taufkirchen, Germany) were added and the samples were incubated in a darkened water quench for 15 min at 37°C (alkylation). For protein digestion, 10 µL trypsin (trypsin/protein ratio: 1/40; Promega, Mannheim, Germany) was added and samples were incubated in a water quench for 16 h at 37°C. Digestion was stopped by addition of 20 µL formic acid (10% v/v; Sigma-Aldrich, Taufkirchen, Germany). All samples were stored at -80°C until further processing. The samples were centrifuged one more time for 15 min at 16 000 g and 4°C. Finally, 50 µL of the supernatant was mixed with 25 µL isotope-labeled internal standard (IS) peptide mix (10 nM of each IS; Thermo Fisher Scientific, Dreieich, Germany). All sample preparations and digestion steps were performed using Protein LoBind tubes (Eppendorf, Hamburg, Germany). Protein quantification was conducted on a 5500 QTRAP triple quadrupole mass spectrometer (AB Sciex, Darmstadt, Germany) coupled to an Agilent Technologies 1260 Infinity system (Agilent Technologies, Waldbronn, Germany) using validated LC-MS/MS methods as recently described (Gröer et al., 2013). The monitored peptides for OATP1B3 were ISITQIER, IYNSVFFGR and NVTGFFQSLK while LSLDELHR was used for Na/K-ATPase. For each peptide, 3-4 mass transitions have been monitored and the absolute protein abundance was assessed by using the stable isotope method and considering the protein content of the sample (data given as pmol transporter protein per mg membrane protein).

2.11. Cellular uptake assays

Molecular Pharmacology Fast Forward. Published on September 27, 2022 as DOI: 10.1124/molpharm.122.000539
This article has not been copyedited and formatted. The final version may differ from this version.

Uptake experiments were performed as described earlier (König et al., 2012). In brief, cells were seeded at an initial cell number of 7 x 10^5 cells per well on poly-D-lysine coated 12-well plates. After twenty-four hours cells were induced with 10 mM sodium butyrate to obtain higher protein levels. Before uptake experiments, cells were washed with prewarmed uptake buffer (142 mM NaCl, 5 mM KCl, 1 mM K_2HPO_4, 1.2 mM $MgSO_4$, 1.5 mM $CaCl_2$, 5 mM glucose and 12.5 mM HEPES, pH 7.3). Radiolabelled substrates were dissolved in uptake buffer and unlabelled substances were added in the respective concentrations for the uptake experiments [BSP (1 µM) and $E_2$17βG (5 µM)]. The cells were incubated with the uptake solution for 10 min and subsequently washed three-times with ice-cold uptake buffer. After the cells were lyzed with 0.2 % SDS, the intracellular accumulation of radioactivity was determined by liquid scintillation counting and protein concentrations were determined by a bicinchoninic acid assay (BCA Protein Assay Kit, Thermo Fisher Scientific, Bonn Germany). The uptake of 2 µM OG was measured accordingly (without radiolabelled OG) and intracellular OG was measured using the CLARIOstar (BMG LABTECH GmbH, Ortenberg, Germany) after 10 min incubation by pipetting 100 µL of each cell lysate and an Oregon Green™ dilution series in 0.2% SDS solution into a 96-well plate. The emission was measured using the preinstalled fluorescein settings.

2.12. Colocalization analysis

For colocalization analysis, µ-Slide 8-well glass bottom arrays (ibidi GmbH, Gräfeling, Germany) were used and coated with 200 µL poly-D-lysine. Next, 9 x 10^4 HEK-Kz-Ct-OATP1B3 cells per well were seeded into the µ-Slide and incubated for 24 h at 37°C and 5% CO_2. Afterwards, either 20 µL of the CellLight™ lysosomes RFP, BacMam 2.0 solution per well was added or the cells were transfected with the pmScarlet-1_peroxisome_C1 plasmid by lipofection and incubated overnight. Finally, the cells

Molecular Pharmacology Fast Forward. Published on September 27, 2022 as DOI: 10.1124/molpharm.122.000539
This article has not been copyedited and formatted. The final version may differ from this version.

were incubated with 1 µM OG solution for 1 h, washed with PBS and subsequently, 200 µL new culture medium was applied. OG-fluorescence was measured using the preinstalled settings of the GFP channel, SPY555 was measured using the Cy3 channel of the Zen software (RRID:Addgene_85065, Carl Zeiss Microscopy GmbH, Jena, Germany). Microscopy was performed on the Zeiss Spinning Disc Axio Observer Z1 (Carl Zeiss Microscopy GmbH, Jena, Germany) at the OICE (Erlangen, Germany).

2.13. Cytotoxicity analysis

7 x 10^3 cells per well were seeded on poly-D-lysine coated 96-well plates at a volume of 200 µL (for DLD1 cells 4 x 10^3 cells at 100 µL/well). After 24 h, the kinase inhibitors (stock solutions dissolved in DMSO) were added to the respective cell culture medium. Cells were incubated for 72 h after compound addition. For vemurafenib and regorafenib the medium was removed and the wells were carefully washed twice with 200 µL PBS solution. To lyse the cells,100 µL of 0.2% SDS solution were added to each well and the plate was shaken for 30 min on a 96-well plate shaker. After the lysis, 150 µL BCA solution was added and the plate was incubated for 30 min at 37°C. The absorption was measured at 560 nm using a Multiskan™ FC multiplate reader (Thermo Fisher Scientific inc., Waltham, USA). The blank value was subtracted and the absorption values were normalized with the average value of the control. Because encorafenib was interacting with the BCA assay, the CCK-8 assay was used to determine cytotoxicity. For this purpose,10 µL CCK-8 substrate per well were added to the cells after 72 h of compound treatment and incubated for 2 h at 37°C. The absorption was measured at 450 nm and normalized to the average absorption of the untreated cells. BSP was used as Ct-OATP1B3 transport inhibitor at 200 µM and was added additionally with the cytotoxic

Molecular Pharmacology Fast Forward. Published on September 27, 2022 as DOI: 10.1124/molpharm.122.000539
This article has not been copyedited and formatted. The final version may differ from this version.

compounds and the respective absorption values were normalized to the average absorption of cells treated with BSP only.

2.14. Quantification of encorafenib in the lysosomal fraction by mass spectrometry

DLD1 cells were seeded at 1 x 10^7 cells on 10 cm plates. The cells were incubated either with 100 µM encorafenib alone or in combination with 200 µM BSP for 4 h. Subsequently, the lysosomal fraction was enriched as described above with minor modifications. The lysosomal pellet was first resuspended in 50 µL PBS and 2.5 µL of this suspension was used to determine the protein amount via BCA assay. The samples were again centrifuged for 10 min at 17 000 x g and 4°C and the PBS was removed. Each pellet was lysed in 80% MeOH/Water (including the internal standard [$^2H_3$]-clopidogrel) and afterwards centrifuged for 10 min at 25 000 x g at 4°C and 200 µL of the supernatant was transferred into HPLC insert glass vials. The solvent was evaporated using a MULTIVAP® nitrogen evaporator (Organomation®, Berlin, MA, USA) and the residue was reconstituted in 100 µL solution with 90% water (containing 0.5% formic acid) and 10% MeOH (with 0.1% formic acid). The samples were measured in triplicates via an in-house method with a Q-Exactive™ Focus mass spectrometer coupled to a Dionex UltiMate™ 3000 ultra-high performance liquid chromatography (UHPLC), (both Thermo Fisher Scientific, Dreieich, Germany) (Kehl et al., 2021). The area of the encorafenib peak was normalized to the peak area of the internal standard and to the protein amount of the lysosomal fraction aliquot. The data are given as % of the average amount of encorafenib in the DLD1 cells without added BSP.

2.15. Statistical analysis

For all transport and cytotoxicity studies at least two independent experiments were performed on different days each measured in triplicates or quadruplets. All data are

Molecular Pharmacology Fast Forward. Published on September 27, 2022 as DOI: 10.1124/molpharm.122.000539
This article has not been copyedited and formatted. The final version may differ from this version.

expressed as means ± SD. The graphs and statistical analysis were done by using GraphPad Prism (RRID:SCR_002798; Version 5.01, 2007, GraphPad Software, San Diego, CA, USA). The statistical significance was analyzed using either One-way ANOVA with Bonferroni adjusted post hoc tests (comparison between all pairs of columns; group size = 4, if more than two cell lines were used) or a two-tailed unpaired student`s t-test (comparison between two cell lines). For cytotoxicity experiments p-values were calculated for each tested kinase inhibitor concentration to demonstrate statistically different effects between HEK-VC control cells and HEK-Kz-Ct-OATP1B3 cells. Due to the exploratory design of the experiment the calculated p-values are descriptive.

3. Results

3.1. Establishment of cell lines recombinantly overexpressing OATP1B3 variants

Ct-SLCO1B3 cDNA was cloned by an RT-PCR-based approach using human colon cancer total RNA as template. The cDNA was inserted into the expression vector pcDNA3.1Hygro(-) resulting in the plasmid pCt-SLCO1B3.31_Hygro. Because it has been demonstrated that a Kozak consensus sequence around the start codon of the *Ct-SLCO1B3* cDNA enhances protein expression (Imai et al., 2013), the original cDNA was mutated to contain a Kozak consensus sequence, resulting in the plasmid pKz-Ct-SLCO1B3.31_Hygro. Both plasmids were used to establish HEK293 cells recombinantly overexpressing the identical Ct-OATP1B3 protein (HEK-Ct-OATP1B3 and HEK-Kz-Ct-OATP1B3). *SLCO1B3* mRNA expression analysis was performed by qRT-PCR (Figure 2A) showing an expression of 21.9 ± 3.04% and 56.8 ± 0.7% in HEK-Ct-OATP1B3 and HEK-Kz-Ct-OATP1B3 cells, respectively (normalized to the expression of the housekeeping gene *β-actin*). Already established HEK293 cells recombinantly overexpressing the liver-type variant of the OATP1B3 protein (HEK-Lt-

Molecular Pharmacology Fast Forward. Published on September 27, 2022 as DOI: 10.1124/molpharm.122.000539
This article has not been copyedited and formatted. The final version may differ from this version.

OATP1B3) had a *SLCO1B3* mRNA expression of 119.7 ± 11.7% relative to the expression of *β-actin* (Seithel et al., 2007).

Immunoblot analysis using whole cell homogenates (Figure 2B) demonstrated a fully glycosylated OATP1B3 protein in HEK-Lt-OATP1B3 cells, whereas in both cell lines expressing the Ct-OATP1B3 protein a weak band was detectable around 75 kDa representing the core-glycosylated form of the OATP1B3 protein (König et al., 2000). In the manuscript by König and coworkers the same antiserum was used. By using confocal laser scanning microscopy (Figure 2C) we could confirm the known localization of the Lt-OATP1B3 (red staining) in the plasma membrane (sodium-potassium ATPase, green staining) of HEK-Lt-OATP1B3 cells, whereas in both cell lines expressing the Ct-OATP1B3 protein (red staining), a more intense intracellular staining could be detected in comparison to HEK-VC.

3.2. Cellular uptake assays

To investigate the function of the OATP1B3 proteins as uptake transporters (putatively) localized in the plasma membrane, cellular uptake assays (Taghikhani et al., 2017) were performed using the prototypic OATP1B3 substrates bromosulfophthalein (BSP; Figure 3A), estradiol-17β-glucuronide ($E_2$17βG; Figure 3B) and Oregon Green™ 488 (OG; Figure 3C). All three substrates had a markedly higher uptake into HEK-Lt-OATP1B3 cells ($P < 0.001$ vs. uptake into HEK-VC cells), but no differences in the uptake of HEK-Ct-OATP1B3 and HEK-Kz-Ct-OATP1B3 cells could be detected compared to the uptake into HEK-VC control cells.

3.3. Proteomics analysis

Using a proteomics analysis, the OATP1B3 protein amount in the isolated plasma membrane fraction (Figure 4A) and in the crude membrane fraction (Figure 4B) of the

Molecular Pharmacology Fast Forward. Published on September 27, 2022 as DOI: 10.1124/molpharm.122.000539
This article has not been copyedited and formatted. The final version may differ from this version.

HEK293 cells was quantified. In the isolated plasma membrane fractions OATP1B3 protein could be detected in HEK-Lt-OATP1B3 cells, but not in HEK-VC, HEK-Ct-OATP1B3 and HEK-Kz-Ct-OATP1B3 (Figure 4A). In the crude membrane fractions of HEK-Ct-OATP1B3 and HEK-Kz-Ct-OATP1B3 cells OATP1B3 protein could be detected, but not in HEK-VC cells (Figure 4B). Due to the high protein amount the quantification of Lt-OATP1B3 protein was omitted in the crude membrane fraction.

3.4. Subcellular localization of Ct-OATP1B3

For subsequent experiments, only HEK-Kz-Ct-OATP1B3 cells were used as Ct-OATP1B3 overexpressing cells because of the higher *SLCO1B3* mRNA expression. Next, the subcellular localization of the Ct-OATP1B3 protein was analyzed. In immunoblot analysis and in line with the proteomics analysis, there was no detectable protein band at 75 kDa in the isolated plasma membrane fraction of the HEK-Kz-Ct-OATP1B3 cells. However, a band could be detected in the cytosolic fraction containing intracellularly localized organelles (Figure 4C). In contrast, a strong band at 130 kDa could be detected in HEK-Lt-OATP1B3 cells, whereas no protein was detectable in the cytosolic fraction of these cells. Next, we isolated the lysosomal fraction of HEK-Kz-Ct-OATP1B3 and HEK-VC cells and analyzed the protein abundance. Figure 4D shows an OATP1B3 protein band at 75 kDa in the enriched lysosomal fraction. Because the OATP1B3 staining using the polyclonal antiserum SKT also leads to unspecific protein binding (e.g. the protein bands in the cytosolic and lysosomal fractions at approx. 65 kDa) and the fact, that no monoclonal anti-OATP1B3 antibody, which is able to detect both variants, is commercially available, a direct colocalization with lysosomal markers was not possible (data not shown). Therefore, we tried to confirm the lysosomal localization by transfecting the HEK-Kz-Ct-OATP1B3 cells either with the baculovirus-based CellLight® lysosomes-

Molecular Pharmacology Fast Forward. Published on September 27, 2022 as DOI: 10.1124/molpharm.122.000539
This article has not been copyedited and formatted. The final version may differ from this version.

RFP, BacMam 2.0 system to stain the lysosomes or with the pmScarlet-1_peroxisome_C1 plasmid to stain the peroxisomes. Twenty-four hours after transfection, we incubated the cells for 1 h with OG, a known substrate of Lt-OATP1B3 (Fig. 3C) (Izumi et al., 2016). Colocalization of the lysosomal marker with OG, resulting in a yellow color of the lysosomes, could be detected (Figure 4E), whereas no colocalization could be detected between OG stained vesicles and the stained peroxisomes (Figure 4F, Figure S1), indicating lysosomal localization of the Ct-OATP1B3 protein.

3.5. Cytotoxicity of kinase inhibitors

To investigate the function of Ct-OATP1B3 localized in lysosomes we used the BRAF inhibitors vemurafenib, substrate and inhibitor of Lt-OATP1B3 (Kayesh et al., 2021; Zimmerman et al., 2013) and encorafenib, approved for the treatment of metastatic colorectal cancer in combination with cetuximab. In addition, we used the VEGFR inhibitor regorafenib (also approved for the treatment of metastatic colorectal cancer), which is not a substrate or inhibitor of Lt-OATP1B3 (FDA, 2013; Ohya et al., 2015). HEK-Kz-Ct-OATP1B3 and HEK-VC cells were incubated with the respective kinase inhibitor at different concentrations and the number of surviving cells was determined (Figure 5).

Expression of the Ct-OATP1B3 protein led to a better survival when cells were incubated with encorafenib (Figure 5A). A slight effect of Ct-OATP1B3 expression was detected for vemurafenib (Figure 5B; $P = 0.051$ at 100 µM), whereas the survival curves of both cell lines were nearly identical when treated with regorafenib (Figure 5C). This indicates that Ct-OATP1B3 expression may confer resistance against kinase inhibitors and that this resistance is substrate dependent.

3.6. Ct-OATP1B3 in the colorectal cancer cell lines DLD1 and T84

Molecular Pharmacology Fast Forward. Published on September 27, 2022 as DOI: 10.1124/molpharm.122.000539
This article has not been copyedited and formatted. The final version may differ from this version.

Additionally, the *Ct-SLCO1B3* mRNA and Ct-OATP1B3 protein analysis were performed in the two colorectal carcinoma cell lines T84 and DLD1. Both cell lines endogenously express *Ct-SLCO1B3* mRNA (Figure 6A). Furthermore, Ct-OATP1B3 protein expression could be verified in immunoblot (Figure 6B) and proteomics analysis (Figure 6C). The protein band of Ct-OATP1B3 could also be detected in the enriched lysosomal fractions of both cell lines (Figure 6D).

In DLD1 cells, we inhibited the potential Ct-OATP1B3-mediated substrate transport into lysosomes in the cytotoxicity assays by adding the OATP1B3 substrate bromosulfophthalein (BSP, 200 µM). When added in combination with the same kinase inhibitors used in HEK293 cell experiments, BSP led to an increase in the cytotoxic effects of encorafenib (Figure 7A) and vemurafenib (Figure 7B). Interestingly, for regorafenib the addition of BSP led to a markedly higher survival in the DLD1 cells ($P < 0.001$ at 100 µM; Figure 7C). To verify, whether the increase in the cytotoxicity of encorafenib is due to an inhibition of the lysosomal sequestration, we incubated DLD1 cells with encorafenib (100 µM) alone or in combination with BSP for 4 h, isolated the enriched lysosomal fraction and quantified the amount of this kinase inhibitor. Due to transport inhibition, the addition of BSP led to a reduction of encorafenib in the enriched lysosomal fraction ($P < 0.001$, Figure 7D).

4. Discussion

The aim of this study was to gain insights into the expression, localization, and function of the Ct-OATP1B3 protein and to clarify previously published inconsistent results regarding these issues. Therefore, we established stably-transfected HEK293 cells recombinantly overexpressing this transport protein and investigated protein amount and localization, Ct-OATP1B3-mediated transport, and a possible function of Ct-OATP1B3 expression in transfected HEK293 cells and colorectal cancer cells. Our

Molecular Pharmacology Fast Forward. Published on September 27, 2022 as DOI: 10.1124/molpharm.122.000539
This article has not been copyedited and formatted. The final version may differ from this version.

results demonstrate that Ct-OATP1B3 protein is localized in lysosomes mediating the transport of substances into these intracellular vesicles. Furthermore, expression of Ct-OATP1B3 protein led to a better survival of cells when treated with the kinase inhibitor encorafenib used for the treatment of metastatic colorectal cancer.

Before Nagai et al. (Nagai et al., 2012) characterized the *Ct-SLCO1B3*-mRNA as a splice variant of the *SLCO1B3* gene expressed in colorectal cancer tissue, several authors described OATP1B3 overexpression in different cancerous tissues without discriminating between the Lt- and Ct-OATP1B3 variant (Abe et al., 2001; Lee et al., 2008; Lockhart et al., 2008). Hence, these older studies may need re-evaluation on this background, and further studies should discriminate between both variants (Alam et al., 2018; Sun et al., 2020). For example, Alam et al. (Alam et al., 2018) identified mRNA expression of both variants in breast cancer samples, whereas Thakkar et al. detected only *Ct-SLCO1B3*-mRNA in CRC samples (Thakkar et al., 2013). This discrimination of both variants could also help to explain the described varying *SLCO1B3*-correlated outcomes in breast cancer (Muto et al., 2007; Tang et al., 2021) and CRC (Teft et al., 2015; Zhi et al., 2021). Furthermore, the published results obtained with CRC cells transfected with the cDNA encoding the Lt-OATP1B3 protein (Lee et al., 2008; Niedermeyer et al., 2014) are difficult to interpret because the localization of Ct-OATP1B3 is altered due to the truncated aminoterminal end (Chun et al., 2017). This altered localization of the Ct-OATP1B3 protein could be verified with the present work, since no Ct-OATP1B3 protein could be detected in the isolated plasma membrane fraction (Figure 4A), but low amounts were detectable in the crude membrane fraction (Figure 4B). In addition, this aminoterminal truncation seems to affect the glycosylation of the Ct-OATP1B3 protein (Figure 2B) resulting in a band with a molecular weight of approximately 75 kDa (Ho et al., 2006; König et al., 2000).

Molecular Pharmacology Fast Forward. Published on September 27, 2022 as DOI: 10.1124/molpharm.122.000539
This article has not been copyedited and formatted. The final version may differ from this version.

Similar results were obtained by analyzing Ct-OATP1B3 expression in the colorectal carcinoma cell line HCT-116 and the pancreatic cancer cell line Panc-1 (Thakkar et al., 2013) and by analyzing the N-linked glycosylation of Lt-OATP1B3 in nonalcoholic fatty liver disease (Clarke et al., 2017). Additionally, the results of the cellular uptake experiments (Figure 3), which showed no difference between the Ct-OATP1B3 transfectants and HEK-VC, are in line with the intracellular localization of Ct-OATP1B3 and with the previously described lack of transport function (Thakkar et al., 2013).

Because unspecific antiserum binding of the polyclonal antiserum SKT and the low protein translation efficiency, especially in stably-transfected HEK293 cells, limit the methods of protein detection, colocalization studies were used to identify the vesicles containing the Ct-OATP1B3 protein. Using the fluorescent dye and known OATP1B3 substrate OG, we analyzed the potential transport function of Ct-OATP1B3 protein located in intracellular vesicles (Figure 4E-F) and identified these vesicles as lysosomes by co-transfection with the lysosomal marker BacMam Lysosomes-RFP (Figure 4E). Interestingly, this lysosomal localization may be of special interest for the possible function of Ct-OATP1B3 protein expression in cancer cells. Lysosomal sequestration has been described for various drugs used in antitumor therapy, especially some kinase inhibitors (e.g. nintendanib, sunitinib) (Krchniakova et al., 2020). This sequestration leads to a reduced cytoplasmic concentration of these drugs and consequently results in a higher cytotoxic resistance (Englinger et al., 2017). So far, this kind of transport has been attributed to the function of ABC-transporters [e.g. ABCA3, P-glycoprotein] localized in lysosomal membranes (Chapuy et al., 2009; Yamagishi et al., 2013). Our cytotoxicity experiments (Figure 5) demonstrated that overexpression of the SLC transporter Ct-OATP1B3 led to a better

Molecular Pharmacology Fast Forward. Published on September 27, 2022 as DOI: 10.1124/molpharm.122.000539
This article has not been copyedited and formatted. The final version may differ from this version.

survival of cells when incubated with selected kinase inhibitors suggesting that also SLC transporters located in intracellular vesicles may be important for this resistance mechanism.

Zimmermann et al. could demonstrate a considerably higher uptake of vemurafenib into stable-transfected HEK293 cells overexpressing Lt-OATP1B3, compared to the HEK293 control cell line (Zimmerman et al., 2013). The other BRAF inhibitor encorafenib is not described as substrate for the Lt-OATP1B3 protein so far and did not show an enhanced uptake into HEK-Lt-OATP1B3 cells compared to the control cell line in our experiments (Figure S2), but both BRAF inhibitors are mentioned as inhibitors of Lt-OATP1B3-mediated transport by the Food and Drug Administration (FDA, 2011; FDA, 2018). Notably, the tested concentrations of vemurafenib in this study were in the concentration range of its reported plasma trough concentrations in humans (Mueller-Schoell et al., 2021; Verheijen et al., 2017), underlining a potential in vivo relevance of Ct-OATP1B3. This was recently reported for OATP1B3 protein, without discriminating between the Lt- and Ct-OATP1B3 protein (Kayesh et al., 2021). It should be noted that the cytoprotective effect of Ct-OATP1B3 expression is not a general effect for all kinase inhibitors as we could show with regorafenib, which is neither a substrate nor inhibitor of Lt-OATP1B3 (Figure 5C) (FDA, 2013; Ohya et al., 2015). Interestingly, the protective effect of Ct-OATP1B3 expression was diminished by the co-application of the Lt-OATP1B3 substrate BSP together with encorafenib (Figure 7A) or vemurafenib (Figure 7B) in DLD1 cells endogenously expressing Ct-OATP1B3. In this experimental setup, the Ct-OATP1B3-mediated transport of both kinase inhibitors into lysosomes seems to be inhibited, resulting in an increased cytotoxicity of treated DLD1 cells. In line with these results, the amount of encorafenib in the enriched lysosomal fraction was reduced (Figure 7D). It can be

Molecular Pharmacology Fast Forward. Published on September 27, 2022 as DOI: 10.1124/molpharm.122.000539
This article has not been copyedited and formatted. The final version may differ from this version.

speculated that Ct-OATP1B3-mediated resistance could contribute to insufficient clinical effects of monotherapy of BRAF-inhibitors in colorectal cancer (Mao et al., 2013; Prahallad et al., 2012; Yaeger et al., 2017).

Taken together, we could demonstrate that Ct-OATP1B3 protein, a splice variant of the liver-type uptake transporter Lt-OATP1B3 is localized in lysosomes and is capable of transporting Ct-OATP1B3 substrates into these vesicles. Furthermore, as shown for encorafenib, the substrate spectrum between the Ct-OATP1B3 and the Lt-OATP1B3 protein seems to be different and further studies are necessary to gain insights into the substrate spectrum of the Ct-OATP1B3 protein. When treated with kinase inhibitors the expression of Ct-OATP1B3 protein led to a better survival of cells by transporting these cytotoxic compounds into lysosomes, thereby reducing their cytoplasmic concentration. This is a new kind of a Ct-OATP1B3-mediated resistance mechanism against antitumor drugs and in line with the association of a higher *Ct-SLCO1B3* expression and a reduced progression-free survival or overall survival of colorectal cancer patients (Teft et al., 2015; Zhi et al., 2021). Its importance for therapy of other tumor entities expressing Ct-OATP1B3 or for other antitumor drugs which are substrates of this transport protein needs to be elucidated in the future. Furthermore, these results suggest that expression of Ct-OATP1B3 protein in tumor tissues may serve as important biomarker for patients treated with antitumor drugs.

Acknowledgements: We thank Olga Stelmakh and Claudia Hoffmann for their technical assistance. Microscopy analysis was performed with the support of the Optical Imaging Centre Erlangen (OICE) and Dr. Philipp Tripal, Dr. Benjamin Schmidt and Dr. Zoltán Winter. DLD1 and T84 cells were kindly provided by PD Dr. Britzen-Laurent and Prof. Dr. Naschberger (Erlangen, Germany).

Authorship Contributions: Participated in research design: Haberkorn, Oswald, Gessner, Taudte, Zunke, Fromm, König; Conducted experiments: Haberkorn, Oswald, Kehl, Dobert; Contributed new reagents or analytic tools: Oswald, Gessner, Taudte, Dobert, Zunke; Performed data analysis: Haberkorn, Oswald, König; Wrote or contributed to the writing of the manuscript: Haberkorn, Oswald, Kehl, Gessner, Taudte, Dobert, Zunke, Fromm, König.

Data Availability Statement: The original contributions presented in the study are included in the article, further inquiries can be directed to the corresponding author.

References

Abe T, Unno M, Onogawa T, Tokui T, Kondo TN, Nakagomi R, Adachi H, Fujiwara K, Okabe M, Suzuki T, Nunoki K, Sato E, Kakyo M, Nishio T, Sugita J, Asano N, Tanemoto M, Seki M, Date F, Ono K, Kondo Y, Shiiba K, Suzuki M, Ohtani H, Shimosegawa T, Iinuma K, Nagura H, Ito S and Matsuno S (2001) LST-2, a human liver-specific organic anion transporter, determines methotrexate sensitivity in gastrointestinal cancers. *Gastroenterology* **120**(7): 1689-1699.

Al-Abdulla R, Perez-Silva L, Abete L, Romero MR, Briz O and Marin JJG (2019) Unraveling "The Cancer Genome Atlas" information on the role of SLC transporters in anticancer drug uptake. *Expert Rev Clin Pharmacol* **12**(4): 329-341.

Alam K, Farasyn T, Ding K and Yue W (2018) Characterization of liver- and cancer-type-organic anion transporting polypeptide (OATP) 1B3 messenger RNA expression in normal and cancerous human tissues. *Drug Metab Lett* **12**(1): 24-32.

Chapuy B, Panse M, Radunski U, Koch R, Wenzel D, Inagaki N, Haase D, Truemper L and Wulf GG (2009) ABC transporter A3 facilitates lysosomal sequestration of imatinib and modulates susceptibility of chronic myeloid leukemia cell lines to this drug. *Haematologica* **94**(11): 1528-1536.

Chun SE, Thakkar N, Oh Y, Park JE, Han S, Ryoo G, Hahn H, Maeng SH, Lim YR, Han BW and Lee W (2017) The N-terminal region of organic anion transporting polypeptide 1B3 (OATP1B3) plays an essential role in regulating its plasma membrane trafficking. *Biochem Pharmacol* **131**: 98-105.

Clarke JD, Novak P, Lake AD, Hardwick RN and Cherrington NJ (2017) Impaired N-linked glycosylation of uptake and efflux transporters in human nonalcoholic fatty liver disease. *Liver Int* **37**(7): 1074-1081.

Drozdzik M, Busch D, Lapczuk J, Müller J, Ostrowski M, Kurzawski M and Oswald S (2019) Protein abundance of clinically relevant drug transporters in the human liver and intestine: a comparative analysis in paired tissue specimens. *Clin Pharmacol Ther* **105**(5): 1204-1212.

Englinger B, Kallus S, Senkiv J, Heilos D, Gabler L, van Schoonhoven S, Terenzi A, Moser P, Pirker C, Timelthaler G, Jäger W, Kowol CR, Heffeter P, Grusch M and Berger W (2017) Intrinsic fluorescence of the clinically approved multikinase inhibitor nintedanib reveals lysosomal sequestration as resistance mechanism in FGFR-driven lung cancer. *J Exp Clin Cancer Res* **36**(1): 122 doi:10.1186/s13046-017-0592-3.

Fahrmayr C, Fromm MF and König J (2010) Hepatic OATP and OCT uptake transporters: their role for drug-drug interactions and pharmacogenetic aspects. *Drug Metab Rev* **42**(3): 380-401.

Food and Drug Administration. Clinical pharmacology and biopharmaceutics review(s). 2011. Available online: https://www.accessdata.fda.gov/drugsatfda_docs/nda/2011/202429Orig1s000ClinPharmR.pdf (accessed on 08.04.2022).

Food and Drug Administration. Clinical pharmacology and biopharmaceutics review(s). 2013. Available online: https://www.accessdata.fda.gov/drugsatfda_docs/nda/2013/204369Orig1s000ClinPharmR.pdf (accessed on 08.04.2022).

Food and Drug Administration. Multi-discipline review. 2018. Available online: https://www.accessdata.fda.gov/drugsatfda_docs/nda/2018/210496Orig1s000MultidisciplineR.pdf (accessed on 08.04.2022).

Gröer C, Brück S, Lai Y, Paulick A, Busemann A, Heidecke CD, Siegmund W and Oswald S (2013) LC-MS/MS-based quantification of clinically relevant intestinal uptake and efflux transporter proteins. *J Pharm Biomed Anal* **85**: 253-261.

Hamada A, Sissung T, Price DK, Danesi R, Chau CH, Sharifi N, Venzon D, Maeda K, Nagao K, Sparreboom A, Mitsuya H, Dahut WL and Figg WD (2008) Effect of *SLCO1B3* haplotype on testosterone transport and clinical outcome in caucasian patients with androgen-independent prostatic cancer. *Clin Cancer Res* **14**(11): 3312-3318.

Hays A, Apte U and Hagenbuch B (2013) Organic anion transporting polypeptides expressed in pancreatic cancer may serve as potential diagnostic markers and therapeutic targets for early stage adenocarcinomas. *Pharm Res* **30**(9): 2260-2269.

Ho RH, Tirona RG, Leake BF, Glaeser H, Lee W, Lemke CJ, Wang Y and Kim RB (2006) Drug and bile acid transporters in rosuvastatin hepatic uptake: function, expression, and pharmacogenetics. *Gastroenterology* **130**(6): 1793-1806.

Huang KM, Uddin ME, DiGiacomo D, Lustberg MB, Hu S and Sparreboom A (2020) Role of *SLC* transporters in toxicity induced by anticancer drugs. *Expert Opin Drug Metab Toxicol* **16**(6): 493-506.

Imai S, Kikuchi R, Tsuruya Y, Naoi S, Nishida S, Kusuhara H and Sugiyama Y (2013) Epigenetic regulation of organic anion transporting polypeptide 1B3 in cancer cell lines. *Pharm Res* **30**(11): 2880-2890.

Izumi S, Nozaki Y, Komori T, Takenaka O, Maeda K, Kusuhara H and Sugiyama Y (2016) Investigation of fluorescein derivatives as substrates of organic anion transporting polypeptide (OATP) 1B1 to develop sensitive fluorescence-based OATP1B1 inhibition assays. *Mol Pharm* **13**(2): 438-448.

Kayesh R, Farasyn T, Crowe A, Liu Q, Pahwa S, Alam K, Neuhoff S, Hatley O, Ding K and Yue W (2021) Assessing OATP1B1- and OATP1B3-mediated drug-drug interaction potential of vemurafenib using R-value and physiologically-based pharmacokinetic models. *J Pharm Sci* **110**(1): 314-324.

Kehl N, Schlichtig K, Dürr P, Bellut L, Dörje F, Fietkau R, Pavel M, Mackensen A, Wullich B, Maas R, Fromm MF, Gessner A and Taudte RV (2021) An easily expandable multi-drug LC-MS assay for the simultaneous quantification of 57 oral antitumor drugs in human plasma. *Cancers* **13**(24): 6329 doi:doi:10.3390/cancers13246329.

König J, Cui Y, Nies AT and Keppler D (2000) Localization and genomic organization of a new hepatocellular organic anion transporting polypeptide. *J Biol Chem* **275**(30): 23161-23168.

König J, Klatt S, Dilger K and Fromm MF (2012) Characterization of ursodeoxycholic and norursodeoxycholic acid as substrates of the hepatic uptake transporters OATP1B1, OATP1B3, OATP2B1 and NTCP. *Basic Clin Pharmacol Toxicol* **111**(2): 81-86.

Kounnis V, Ioachim E, Svoboda M, Tzakos A, Sainis I, Thalhammer T, Steiner G and Briasoulis E (2011) Expression of organic anion-transporting polypeptides 1B3, 1B1, and 1A2 in human pancreatic cancer reveals a new class of potential therapeutic targets. *Onco Targets Ther* **4**: 27-32.

Krchniakova M, Skoda J, Neradil J, Chlapek P and Veselska R (2020) Repurposing tyrosine kinase inhibitors to overcome multidrug resistance in cancer: a focus on transporters and lysosomal sequestration. *Int J Mol Sci* **21**(9) doi:10.3390/ijms21093157.

Lee W, Belkhiri A, Lockhart AC, Merchant N, Glaeser H, Harris EI, Washington MK, Brunt EM, Zaika A, Kim RB and El-Rifai W (2008) Overexpression of OATP1B3 confers apoptotic resistance in colon cancer. *Cancer Res* **68**(24): 10315-10323.

Locher KP (2016) Mechanistic diversity in ATP-binding cassette (ABC) transporters. *Nat Struct Mol Biol* **23**(6): 487-493.

Lockhart AC, Harris E, Lafleur BJ, Merchant NB, Washington MK, Resnick MB, Yeatman TJ and Lee W (2008) Organic anion transporting polypeptide 1B3 (OATP1B3) is overexpressed in colorectal tumors and is a predictor of clinical outcome. *Clin Exp Gastroenterol* **1**: 1-7.

Mao M, Tian F, Mariadason JM, Tsao CC, Lemos R, Jr., Dayyani F, Gopal YN, Jiang ZQ, Wistuba, II, Tang XM, Bornman WG, Bollag G, Mills GB, Powis G, Desai J, Gallick GE, Davies MA and Kopetz S (2013) Resistance to BRAF inhibition in BRAF-mutant colon cancer can be overcome with PI3K inhibition or demethylating agents. *Clin Cancer Res* **19**(3): 657-667.

Mazzulli JR, Xu YH, Sun Y, Knight AL, McLean PJ, Caldwell GA, Sidransky E, Grabowski GA and Krainc D (2011) Gaucher disease glucocerebrosidase and α-synuclein form a bidirectional pathogenic loop in synucleinopathies. *Cell* **146**(1): 37-52.

Moitra K and Dean M (2011) Evolution of ABC transporters by gene duplication and their role in human disease. *Biol Chem* **392**(1-2): 29-37.

Mueller-Schoell A, Groenland SL, Scherf-Clavel O, van Dyk M, Huisinga W, Michelet R, Jaehde U, Steeghs N, Huitema ADR and Kloft C (2021) Therapeutic drug monitoring of oral targeted antineoplastic drugs. *Eur J Clin Pharmacol* **77**(4): 441-464.

Muto M, Onogawa T, Suzuki T, Ishida T, Rikiyama T, Katayose Y, Ohuchi N, Sasano H, Abe T and Unno M (2007) Human liver-specific organic anion transporter-2 is a potent prognostic factor for human breast carcinoma. *Cancer Sci* **98**(10): 1570-1576.

Nagai M, Furihata T, Matsumoto S, Ishii S, Motohashi S, Yoshino I, Ugajin M, Miyajima A, Matsumoto S and Chiba K (2012) Identification of a new organic anion transporting polypeptide 1B3 mRNA isoform primarily expressed in human cancerous tissues and cells. *Biochem Biophys Res Commun* **418**(4): 818-823.

Neul C, Schaeffeler E, Sparreboom A, Laufer S, Schwab M and Nies AT (2016) Impact of membrane drug transporters on resistance to small-molecule tyrosine kinase inhibitors. *Trends Pharmacol Sci* **37**(11): 904-932.

Niedermeyer TH, Daily A, Swiatecka-Hagenbruch M and Moscow JA (2014) Selectivity and potency of microcystin congeners against OATP1B1 and OATP1B3 expressing cancer cells. *PLoS One* **9**(3): e91476 doi:10.1371/journal.pone.0091476.

Ogane N, Yasuda M, Kameda Y, Yokose T, Kato H, Itoh A, Nishino S, Hashimoto Y and Kamoshida S (2013) Prognostic value of organic anion transporting polypeptide 1B3 and copper transporter 1 expression in endometrial cancer patients treated with paclitaxel and carboplatin. *Biomed Res* **34**(3): 143-151.

Ohya H, Shibayama Y, Ogura J, Narumi K, Kobayashi M and Iseki K (2015) Regorafenib is transported by the organic anion transporter 1B1 and the multidrug resistance protein 2. *Biol Pharm Bull* **38**(4): 582-586.

Pizzagalli MD, Bensimon A and Superti-Furga G (2021) A guide to plasma membrane solute carrier proteins. *FEBS J* **288**(9): 2784-2835.

Prahallad A, Sun C, Huang S, Di Nicolantonio F, Salazar R, Zecchin D, Beijersbergen RL, Bardelli A and Bernards R (2012) Unresponsiveness of colon cancer to BRAF(V600E) inhibition through feedback activation of EGFR. *Nature* **483**(7387): 100-103.

Pressler H, Sissung TM, Venzon D, Price DK and Figg WD (2011) Expression of OATP family members in hormone-related cancers: potential markers of progression. *PLoS One* **6**(5): e20372 doi:10.1371/journal.pone.0020372.

Robey RW, Pluchino KM, Hall MD, Fojo AT, Bates SE and Gottesman MM (2018) Revisiting the role of ABC transporters in multidrug-resistant cancer. *Nat Rev Cancer* **18**(7): 452-464.

Roth M, Obaidat A and Hagenbuch B (2012) OATPs, OATs and OCTs: the organic anion and cation transporters of the *SLCO* and *SLC22A* gene superfamilies. *Br J Pharmacol* **165**(5): 1260-1287.

Seithel A, Eberl S, Singer K, Auge D, Heinkele G, Wolf NB, Dörje F, Fromm MF and König J (2007) The influence of macrolide antibiotics on the uptake of organic anions and drugs mediated by OATP1B1 and OATP1B3. *Drug Metab Dispos* **35**(5): 779-786.

Seithel A, Glaeser H, Fromm MF and König J (2008) The functional consequences of genetic variations in transporter genes encoding human organic anion-transporting polypeptide family members. *Expert Opin Drug Metab Toxicol* **4**(1): 51-64.

Sun R, Ying Y, Tang Z, Liu T, Shi F, Li H, Guo T, Huang S and Lai R (2020) The emerging role of the SLCO1B3 protein in cancer resistance. *Protein Pept Lett* **27**(1): 17-29.

Sun Y, Furihata T, Ishii S, Nagai M, Harada M, Shimozato O, Kamijo T, Motohashi S, Yoshino I, Kamiichi A, Kobayashi K and Chiba K (2014) Unique expression features of cancer-type organic anion transporting polypeptide 1B3 mRNA expression in human colon and lung cancers. *Clin Transl Med* **3**: 37 doi:10.1186/s40169-014-0037-y.

Taghikhani E, Fromm MF and König J (2017) Assays for analyzing the role of transport proteins in the uptake and the vectorial transport of substances affecting cell viability, in *Cell Viability Assays Methods in Molecular Biology* (Gilbert D and Friedrich O eds) pp 123-135, Humana Press, New York, USA.

Taghikhani E, Maas R, Fromm MF and König J (2019) The renal transport protein OATP4C1 mediates uptake of the uremic toxin asymmetric dimethylarginine (ADMA) and efflux of cardioprotective L-homoarginine. *PLoS One* **14**(3): e0213747 doi:10.1371/journal.pone.0213747.

Taghikhani E, Maas R, Taudte RV, Gessner A, Fromm MF and König J (2020) Vectorial transport of the arginine derivatives asymmetric dimethylarginine (ADMA) and L-homoarginine by OATP4C1 and P-glycoprotein studied in double-transfected MDCK cells. *Amino Acids* **52**(6-7): 975-985.

Tang T, Wang G, Liu S, Zhang Z, Liu C, Li F, Liu X, Meng L, Yang H, Li C, Sang M and Zhao L (2021) Highly expressed SLCO1B3 inhibits the occurrence and development of breast cancer and can be used as a clinical indicator of prognosis. *Sci Rep* **11**(1): 631 doi:10.1038/s41598-020-80152-0.

Teft WA, Welch S, Lenehan J, Parfitt J, Choi YH, Winquist E and Kim RB (2015) OATP1B1 and tumour OATP1B3 modulate exposure, toxicity, and survival after irinotecan-based chemotherapy. *Br J Cancer* **112**(5): 857-865.

Thakkar N, Kim K, Jang ER, Han S, Kim K, Kim D, Merchant N, Lockhart AC and Lee W (2013) A cancer-specific variant of the *SLCO1B3* gene encodes a novel human organic anion transporting polypeptide 1B3 (OATP1B3) localized mainly in the cytoplasm of colon and pancreatic cancer cells. *Mol Pharm* **10**(1): 406-416.

Verheijen RB, Yu H, Schellens JHM, Beijnen JH, Steeghs N and Huitema ADR (2017) Practical recommendations for therapeutic drug monitoring of kinase inhibitors in oncology. *Clin Pharmacol Ther* **102**(5): 765-776.

Yaeger R, Yao Z, Hyman DM, Hechtman JF, Vakiani E, Zhao H, Su W, Wang L, Joelson A, Cercek A, Baselga J, de Stanchina E, Saltz L, Berger MF, Solit DB and Rosen N (2017) Mechanisms of acquired resistance to BRAF V600E inhibition in colon cancers converge on RAF dimerization and are sensitive to its inhibition. *Cancer Res* **77**(23): 6513-6523.

Yamagishi T, Sahni S, Sharp DM, Arvind A, Jansson PJ and Richardson DR (2013) P-glycoprotein mediates drug resistance via a novel mechanism involving lysosomal sequestration. *J Biol Chem* **288**(44): 31761-31771.

Zhang Y and Wang J (2020) Targeting uptake transporters for cancer imaging and treatment. *Acta Pharm Sin B* **10**(1): 79-90.

Zhi L, Zhao L, Zhang X, Liu W, Gao B, Wang F, Wang X and Wang G (2021) *SLCO1B3* promotes colorectal cancer tumorigenesis and metastasis through STAT3. *Aging (Albany NY)* **13**(18): 22164-22175.

Zimmerman EI, Hu S, Roberts JL, Gibson AA, Orwick SJ, Li L, Sparreboom A and Baker SD (2013) Contribution of OATP1B1 and OATP1B3 to the disposition of sorafenib and sorafenib-glucuronide. *Clin Cancer Res* **19**(6): 1458-1466.

Molecular Pharmacology Fast Forward. Published on September 27, 2022 as DOI: 10.1124/molpharm.122.000539
This article has not been copyedited and formatted. The final version may differ from this version.

Footnotes

Conflicts of Interest: The authors declare no conflict of interest.

This work was supported by the Wilhelm Sander-Stiftung (Grants 2019.050.1 and 2019.097.1) and by the DFG (Grant INST 90/1048-1 FUGG).

Reprint request: Prof. Dr. Jörg König
Institute of Experimental and Clinical Pharmacology and Toxicology
Clinical Pharmacology and Clinical Toxicology
Friedrich-Alexander-Universität Erlangen-Nürnberg
Fahrstrasse 17
91054 Erlangen
Germany
Joerg.koenig@fau.de
Tel: ++49-9131-8522077
Fax: ++49-9131-8522773

[1] Institute of Experimental and Clinical Pharmacology and Toxicology, Friedrich-Alexander-Universität Erlangen-Nürnberg, Erlangen, Germany

[2] Institute of Toxicology and Pharmacology, Rostock University Medical Center, Rostock, Germany

[3] Department of Molecular Neurology, University Hospital Erlangen, Friedrich-Alexander-Universität Erlangen-Nürnberg, Erlangen, Germany

Molecular Pharmacology Fast Forward. Published on September 27, 2022 as DOI: 10.1124/molpharm.122.000539
This article has not been copyedited and formatted. The final version may differ from this version.

Figure Legends:

Figure 1. Structure of the *SLCO1B3* gene and the encoded two protein variants. A.) Structure of the human *SLCO1B3* gene. The transcriptional start sides of both variants (*Lt-SLCO1B3* and *Ct-SLCO1B3*) are indicated with curved arrows. The white boxes representing the first three exons of the *Lt-SLCO1B3* variant lacking in the *Ct-SLCO1B3* variant. The black box indicates exon 1* within intron 3 of the *SLCO1B3* gene which is alternatively spliced in front of exon 4 of the Lt-SLCO1B3 gene. Exons 4 to 16 (grey boxes) are identical for the *Lt-* and the *Ct-SLCO1B3* gene variants. Both start codons (ATG) are depicted below the gene structure with ATG in exon 3 is the start codon for the Lt-OATP1B3 protein and ATG at the beginning of exon 4 is the start codon for the Ct-OATP1B3 protein. The stop codon located in exon 16 is identical for both variants. The gene bank entry NM_019844.4 served as reference sequence for the *Lt-SLCO1B3* mRNA and the gene bank entry NM_001349920.2 for the *Ct-SLCO1B3* mRNA. B.) Proteins encoded by both gene variants with the Ct-OATP1B3 protein lacking the first 28 amino acids of the Lt-OATP1B3 protein. C.) Schematic 2D-overview over the aminoterminal regions of Lt- and Ct-OATP1B3 predicted by DeepTMHMM-Predictions. TMH = Transmembrane helix.

Figure 2 Characterization of HEK293 cells stably expressing OATP1B3 variants. (A) *SLCO1B3* mRNA expression analysis. Expression is normalized to the expression of the housekeeping gene *β-actin*. VC = HEK293 cells transfected with the empty vector, Lt-OATP1B3 = HEK293 cells recombinantly overexpressing the liver-type variant of OATP1B3, Ct-OATP1B3 = HEK293 cells transfected with the cancer-type variant of OATP1B3, Kz-Ct-OATP1B3 = HEK293 cells recombinantly overexpressing the cancer-type variant of OATP1B3 with a Kozak sequence around the start codon. Data are given as mean ± SD. The experiment has been performed

in triplicates. (B) Immunoblot analysis using whole cell homogenates. OATP1B3 was detected using the antiserum SKT, pan cadherin served as loading control. OATP1B3 represents the fully glycosylated form, OATP1B3* the core-glycosylated form. (C) Localization of OATP1B3 variants (red) analyzed by confocal laser scanning microscopy. The sodium-potassium ATPase (green) was used as membrane marker, the nuclei are shown in blue. Yellow color results from the colocalization of the membrane marker with the OATP1B3 protein. In both cell lines expressing the Ct-OATP1B3 protein a more intense intracellular staining compared to the staining in the control cells could be detected. *** $p < 0.001$ Lt-OATP1B3, Kz-Ct-OATP1B3 vs. VC; * $p < 0.05$ Ct-OATP1B3 vs. VC.

Figure 3 Cellular uptake assays using prototypic OATP1B3 substrates. Intracellular accumulation of (A) 1 µM BSP, (B) 5 µM estradiol-17β-glucuronide and (C) 2 µM Oregon Green™ 488 into the stable transfectants. Data are given as mean ± SD. The experiments have been performed twice in triplicates. *** $p < 0.001$ Lt-OATP1B3 vs. VC, Ct-OATP1B3, Kz-Ct-OATP1B3.

Figure 4 Proteomics-based expression analysis and subcellular localization of Ct-OATP1B3. Amount of OATP1B3 protein in (A) the isolated plasma membrane fraction and in (B) preparations of crude membrane fraction of the stable transfectants determined by mass spectrometry. BLQ = amount below limit of quantification. Due to the high protein amount, the quantification of Lt-OATP1B3 protein was omitted in the crude membrane fraction. Experiments were performed once with n = 2. (C) Immunoblot analysis of the plasma membrane fraction and the cytosolic fraction of the stably-transfected HEK293 cells. β-actin served as loading control. OATP1B3 represents the fully glycosylated form, OATP1B3* the core-glycosylated form. (D) Analysis of the enriched lysosomal fraction. The lysosomal

Molecular Pharmacology Fast Forward. Published on September 27, 2022 as DOI: 10.1124/molpharm.122.000539
This article has not been copyedited and formatted. The final version may differ from this version.

marker Lamp1 served as loading control. (E and F) HEK-Kz-Ct-OATP1B3 cells were seeded in a µ-slide 8-well glass bottom array and 24 h after seeding cells were transfected with (E) the CellLight® lysosomes-RFP, BacMam 2.0 system or with (F) the pmScarlet-1_peroxisome_C1 plasmid. One hour prior to the experiments the cells were preincubated with 1 µM OG, a known substrate of OATP1B3. The cells were analyzed via confocal laser scanning microscopy.

Figure 5 Cytotoxicity of kinase inhibitors analyzed in stably-transfected HEK293 cells. Cytotoxicity of (A) encorafenib (two experiments measured in quadruplets), (B) vemurafenib (two experiments measured in quadruplets) and (C) regorafenib (three experiments measured in quadruplets) determined by BCA assay (vemurafenib, regorafenib) or CCK-8 assay (encorafenib) after 72 h of drug exposure. Data are presented as mean ± SD. *** $p < 0.001$ Kz-Ct-OATP1B3 (▲) vs. VC (●); n.s. = not significant.

Figure 6 *Ct-SLCO1B3* mRNA and Ct-OATP1B3 protein expression in the colorectal carcinoma cell lines T84 and DLD1. (A) Quantification of the *Ct-SLCO1B3* mRNA expression in T84 and DLD1 cells. Expression is normalized to the mRNA expression of the housekeeping gene *β-actin* and measured once in triplicates. (B) Ct-OATP1B3 protein expression in T84 and DLD1 cells using whole cell homogenate in the immunoblot analysis and (C) the crude membrane fraction in the proteomics analysis (n = 2). (D) Ct-OATP1B3 protein expression in the enriched lysosomal fraction of the CRC cells. Lamp1 served as lysosomal marker.

Figure 7 Effect of Ct-OATP1B3-mediated transport inhibition in DLD1 cells. Cytotoxicity of (A) encorafenib, (B) vemurafenib and (C) regorafenib in DLD1 cells with (■) and without (●) co-incubation of the cells with BSP (200 µM) measured after 72 h of compound treatment. Experiments were performed twice measured in

Molecular Pharmacology Fast Forward. Published on September 27, 2022 as DOI: 10.1124/molpharm.122.000539
This article has not been copyedited and formatted. The final version may differ from this version.

quadruplets. (D) Quantification of encorafenib in the isolated lysosomal fraction after 4 h drug exposure with and without added BSP (two experiments measured in triplicates). *** $p < 0.001$ DLD1 vs. DLD1 + BSP; ** $p < 0.01$ DLD1 vs. DLD1 + BSP; * $p < 0.05$ DLD1 vs. DLD1 + BSP; n.s. = not significant.

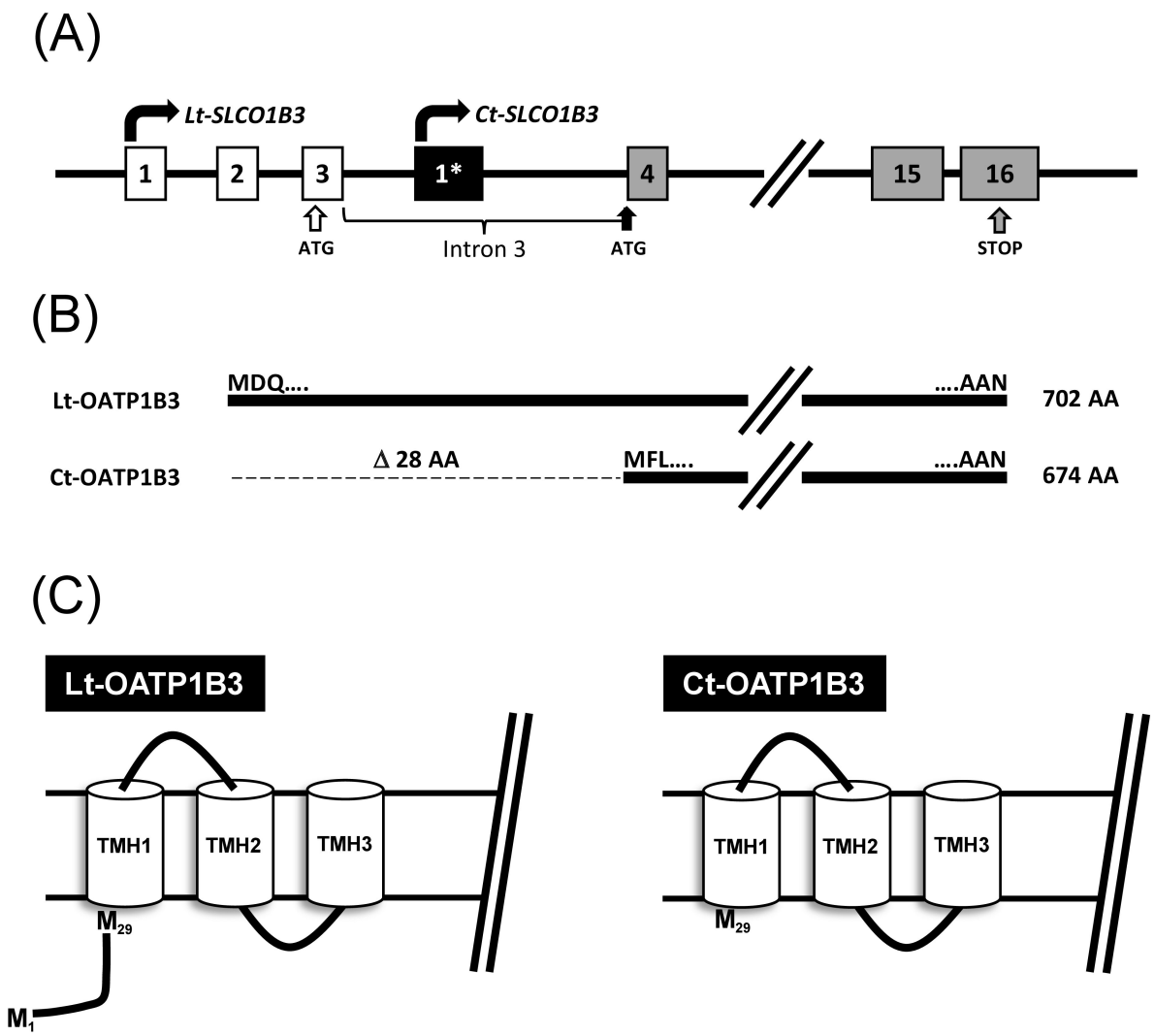

Figure 1

Molecular Pharmacology Fast Forward. Published on September 27, 2022 as DOI: 10.1124/molpharm.122.000535
This article has not been copyedited and formatted. The final version may differ from this version.

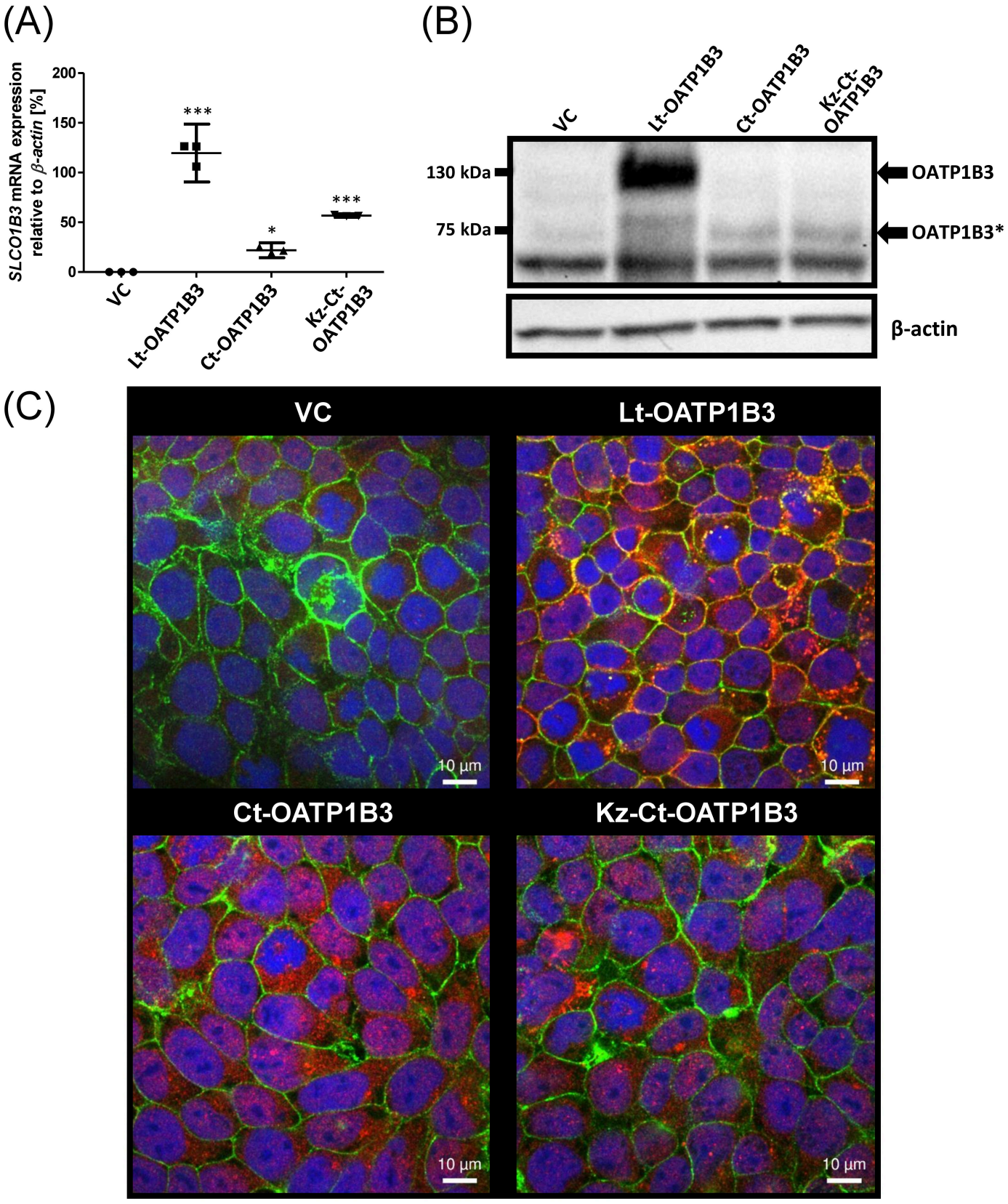

Figure 2

Molecular Pharmacology Fast Forward. Published on September 27, 2022 as DOI: 10.1124/molpharm.122.000535

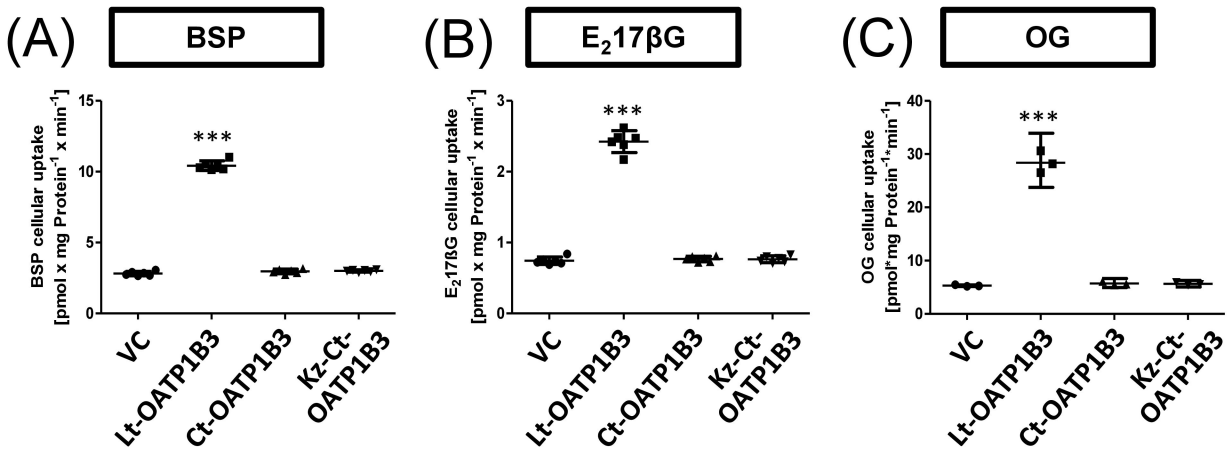

Figure 3

Molecular Pharmacology Fast Forward. Published on September 27, 2022 as DOI: 10.1124/molpharm.122.000535
This article has not been copyedited and formatted. The final version may differ from this version.

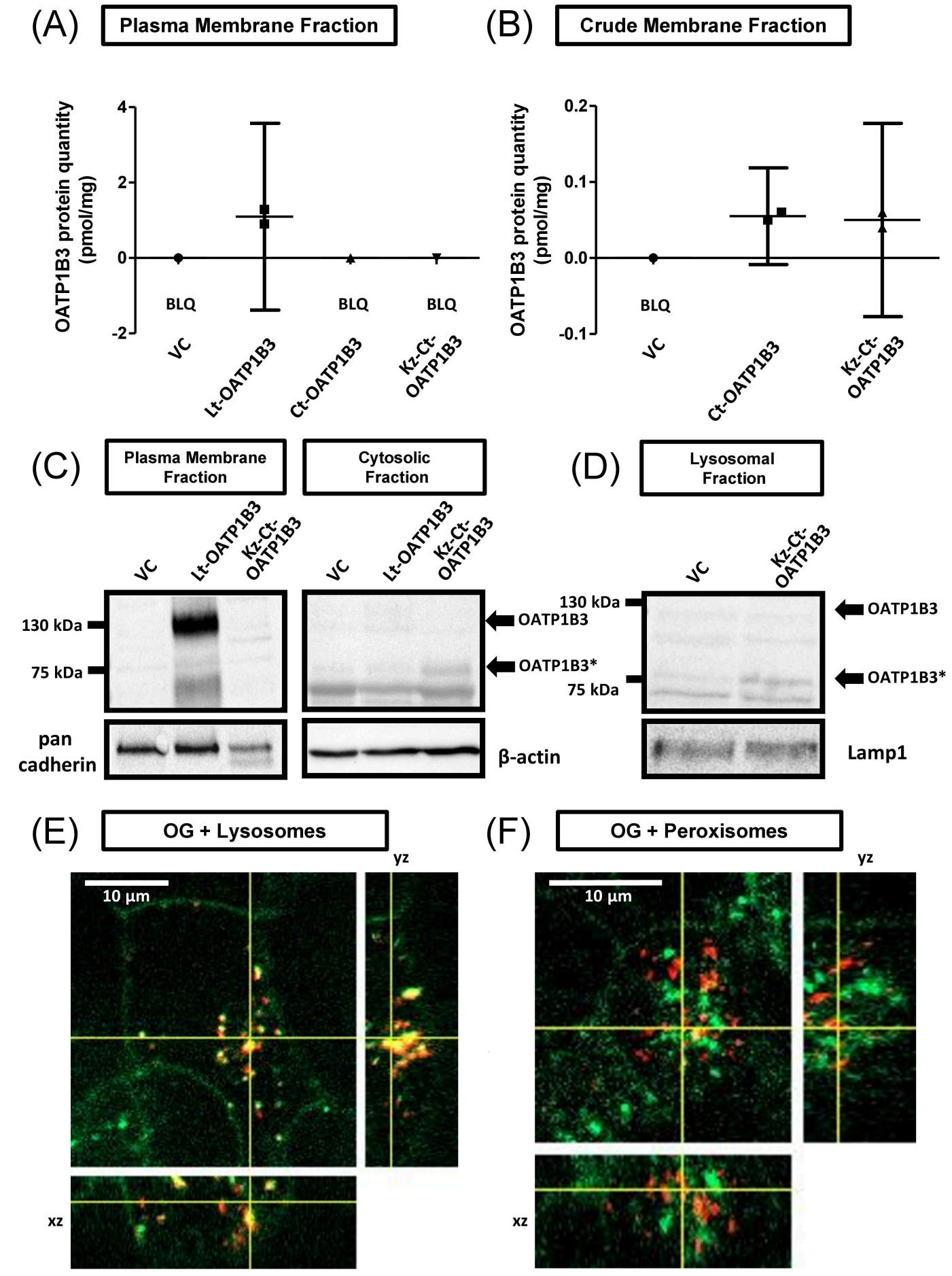

Figure 4

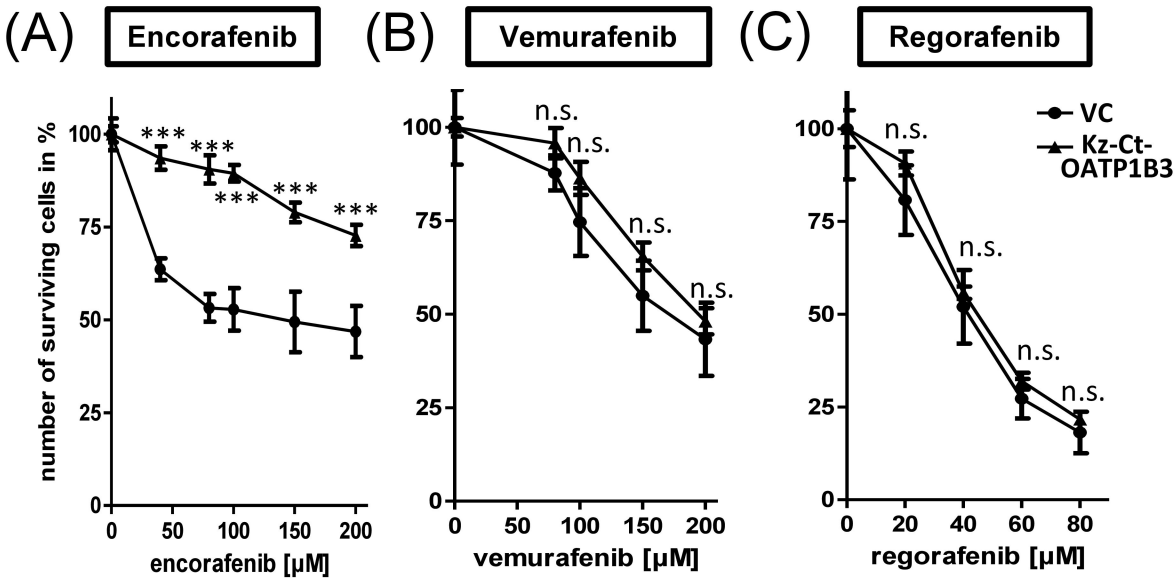

Figure 5

Molecular Pharmacology Fast Forward. Published on September 27, 2022 as DOI: 10.1124/molpharm.122.000535

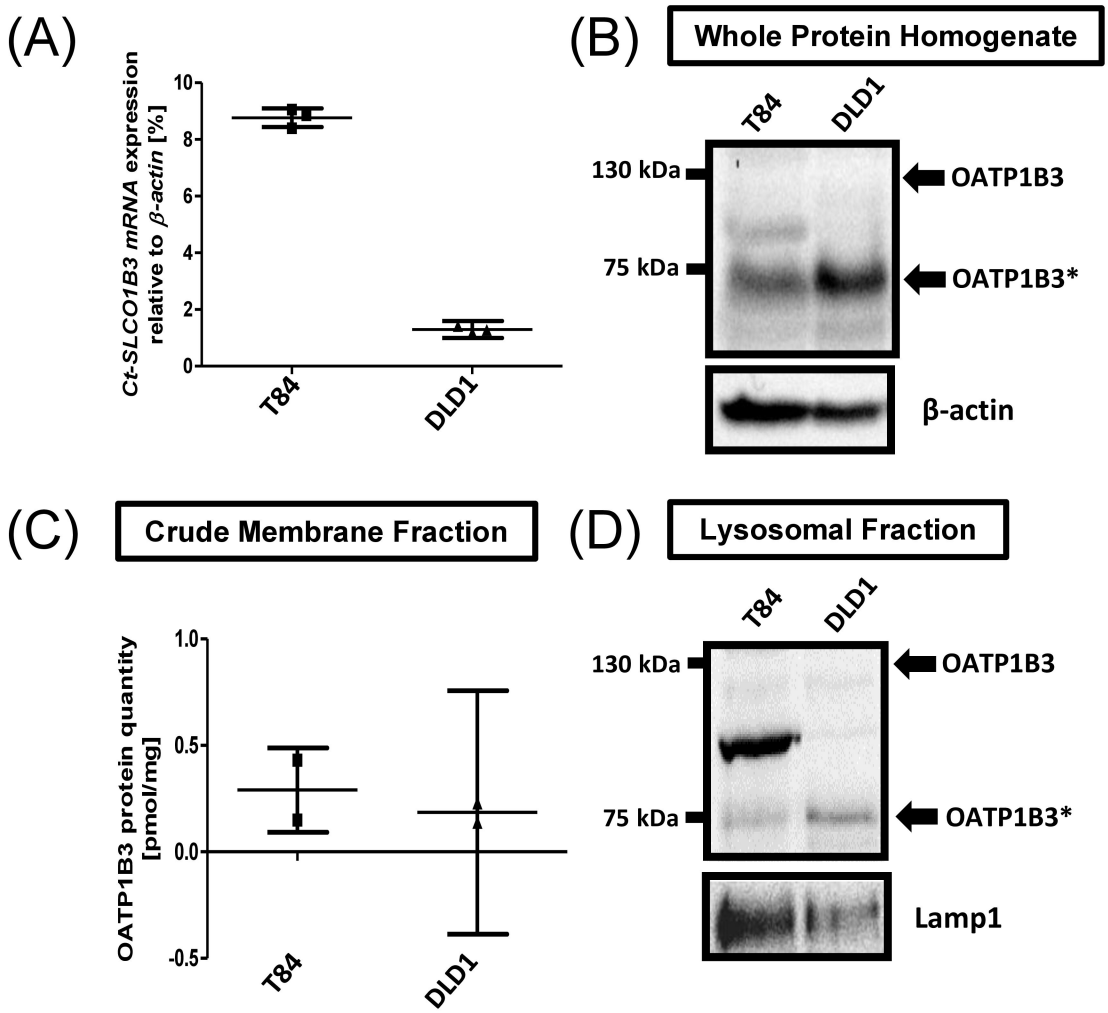

Figure 6

Molecular Pharmacology Fast Forward. Published on September 27, 2022 as DOI: 10.1124/molpharm.122.000535

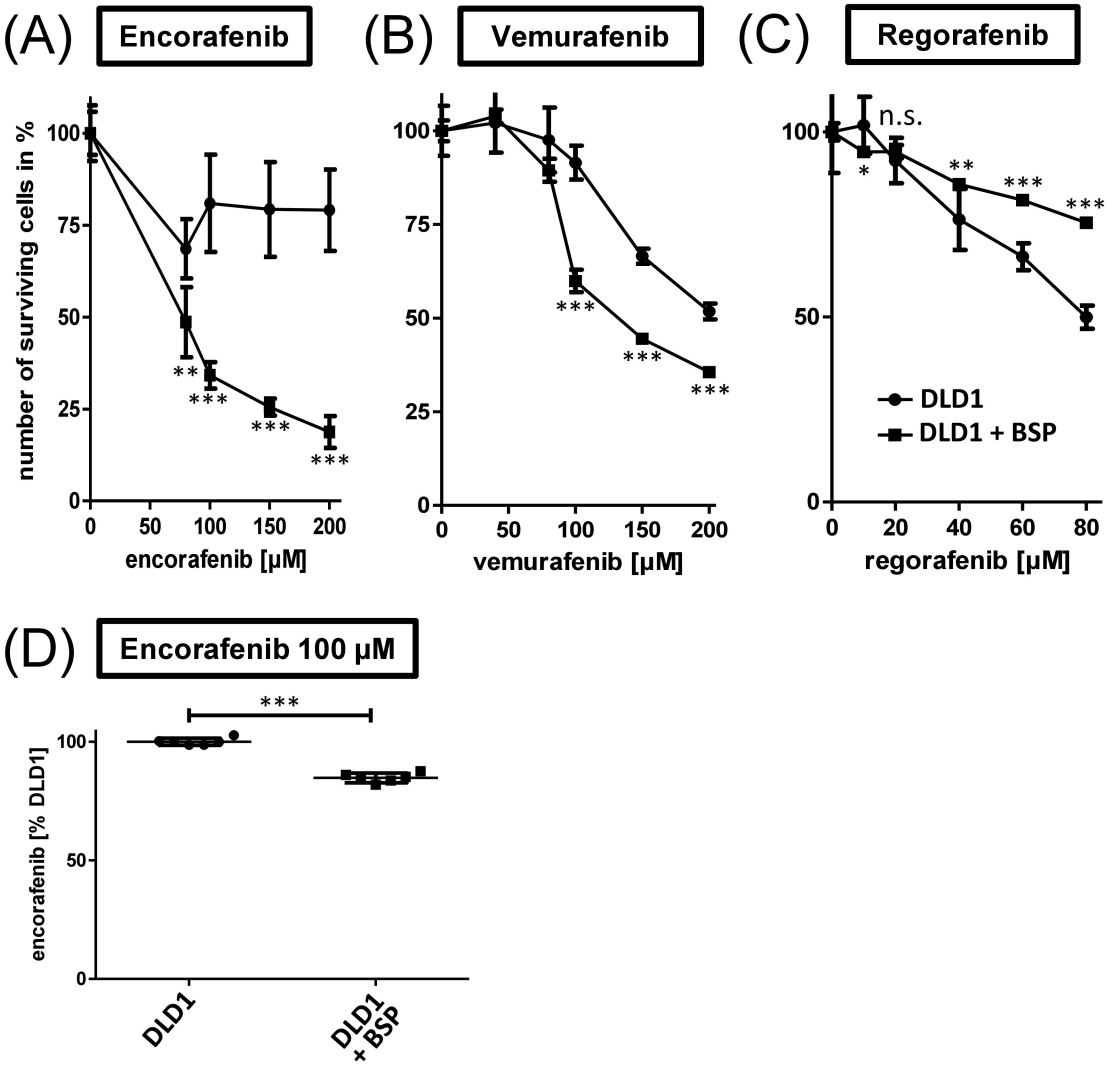

Figure 7